applied sciences

MDPI

Article

Remote Speckle-Based Measurements of Backward Brillouin Acoustic Vibrations in Optical Fibers

Sagie Asraf [1,*], Benjamin Lengenfelder [2,3], Michael Schmidt [2,3] and Zeev Zalevsky [1,*]

1 Faculty of Engineering and the Nano Technology Center, Bar-Ilan University, Ramat-Gan 52900, Israel
2 Institute of Photonic Technologies (LPT), Friedrich-Alexander-Universität Erlangen-Nürnberg (FAU), Konrad-Zuse–Straße 3/5, 91052 Erlangen, Germany; benjamin.lengenfelder@lpt.uni-erlangen.de (B.L.); Michael.Schmidt@lpt.uni-erlangen.de (M.S.)
3 Erlangen Graduate School in Advanced Optical Technologies (SAOT), Paul-Gordan-Straße 6, 91052 Erlangen, Germany
* Correspondence: Sagieas9@walla.co.il (S.A.); Zeev.Zalevsky@biu.ac.il (Z.Z.)

Received: 19 December 2019; Accepted: 15 January 2020; Published: 17 January 2020

check for updates

Abstract: We propose a novel technique for measurements of Brillouin acoustic vibrations based on temporal tracking of back-reflected speckle patterns. The proposed method holds the potential to enhance some of the limiting factors in Brillouin frequency measurements while yielding increased spatial resolution and shorter scanning times of the inspected fiber. Experimental results show the capabilities of the proposed method are presented, using a two pump-waves configuration.

Keywords: brillouin sensing; speckle analysis; fiber sensors

1. Introduction

Stimulated Brillouin scattering (SBS) is a nonlinear effect that was first observed in 1964 [1] and has been studied extensively [2–7]. This effect has been observed in a wide range of liquids [2], gases, and solids [5]. The Brillouin effect was also observed and analyzed in optical fibers, first for the case of stimulated Brillouin scattering [4] and later for the case of spontaneous scattering [8,9]. The Brillouin effect in optical fibers is very useful for several applications like optical filtering [10], amplification of signals [11], and sensing [12].

Brillouin scattering can be described entirely as a coupled three-wave interaction: Two counter-propagating optical waves called pump and Stoke and an acoustic wave. In the case of stimulated Brillouin, both the pump and the Stokes waves are applied externally from both sides of the fiber. The interference between those two generates an acoustic wave within the fiber through a process called electrostriction. The refractive index grating caused by the acoustic wave scatters the pump wave, while the backscattered light is downshifted in its frequency resulting in optical power transfer from the pump wave to the Stokes wave [6,7]. In the case of spontaneous Brillouin, only the pump wave is applied externally. In this case, the acoustic wave which exists within the fiber naturally as a result of thermally generated phonons scatters the pump wave. The back-reflected signal is downshifted in frequency due to the Doppler effect [6]. This shift in frequency called Brillouin frequency and its magnitude depends on the velocity of the acoustic wave, which is proportional to the density of the material in the fiber. Since the density of the material is temperature and strain-dependent, measurement of the Brillouin frequency of the fiber can be used for development of temperature or strain sensors [12].

Currently, the Brillouin frequency measurements are indirectly performed by finding the frequency shift between the injected pump wave and the back-reflected Stokes signal. Several approaches for distributed fiber sensors were suggested in recent years to find the Brillouin frequency in every point along an optical fiber. In the basic method, called Brillouin optical time domain reflectometry (BOTDR), a short pump pulse is inserted into an optical fiber. By measuring the frequency shift of the backscattered light as a function of time, it is possible to find the Brillouin frequency at any point along the fiber [13]. For Brillouin optical time domain analysis (BOTDA), one laser pulse acts as a pump and a second counter-propagated continues wave laser acts as a probe. By measuring the probe amplitude as function of time, and by scanning the frequency difference between the pump and the probe it is possible to find the Brillouin frequency for each point along the fiber [14]. For both mentioned modalities, the spatial resolution is limited to about 1 m by the damping time of the acoustic wave [15]. Several methods were proposed to overcome this spatial resolution limitation like methods that are based on pre-existence of an acoustic wave [16], frequency-domain methods [17,18], Brillouin dynamic grating [19], or correlation-based methods which reach a very high spatial resolution [10–22].

Recently, we proposed a new detection modality based on speckle-sensing for phonon detection in optical fibers [23]. In this method, the acoustic vibrations resulting from the Brillouin effect are directly measured by temporal tracking of the back-reflected secondary speckle patterns, generated while illuminating the tested fiber. This approach holds the potential to improve the spatial resolution for Brillouin scattering detection since it is determined by the size of the illuminated part of the fiber, which can be very small in size (i.e., a few millimeters). Our method also enables us to detect only a specific section of the fiber, without scanning the whole inspected fiber. This property may be significant when we work with long fibers. Moreover, if the field of view of the camera that is capturing the speckle patterns matches to the length of the inspected fiber, then the mapping of the Brillouin frequency along the fiber can be obtained at once without the need to apply time-dependent scanning process. In previous work, we introduced primality results of the detection of Brillouin radial acoustic modes by using this method [23].

In this paper we show for the first time, remote detection of acoustic vibrations in optical fiber resulting from the backward Brillouin effect. Those measurements were performed by using a two pump waves configuration to decrease the frequency of the acoustic vibrations. First, this principle of measurement will be explained in detail. Then we introduce the experimental setup and the received results that show the ability to sense the Brillouin vibrations in an optical fiber by speckles analysis, and finally, we will discuss the meaning of the obtained results.

2. Theoretical Background

2.1. Stimulated Brillouin Scattering

As we mentioned in the introduction, the Brillouin acoustic wave scatters the pump wave while the scattered light will be downshifted in frequency [6,7]. Since the pump wave at frequency ω_p is scattered from a retreating sound wave, the scattered radiation will be shifted downward in frequency to:

$$\omega_s = \omega_p - \Omega_B \tag{1}$$

where ω_s is the backscattered frequency and Ω_B is the acoustic wave frequency, called the Brillouin frequency. Since the Brillouin frequency is related to the acoustic wave vector, and since this wave is driven by the beating of the two counter-propagate pump and Stokes, it is possible to show that the Brillouin frequency is given by [7]:

$$\Omega_B = \frac{2v_a}{c/n}\omega_p \tag{2}$$

where v_a represents the velocity of sound, c is the velocity of light and n is the refractive index of the fiber. Since the acoustic velocity in optical fiber is about 5800 m/s [15], the typical value for Brillouin frequency for pump wave with a wavelength of 1550 nm is about 10 GHz.

2.2. Speckles Analysis

The random self-interference pattern known as speckle, allows us to track changes in the phase of the light being scattered from a rough surface while being illuminated and vibrated [24,25]. By tracking the position of the time-varying correlation peak, it is possible to extract the movement trajectory. In this way, very small temporal shifts and movements of an object can be measured [16]. The shift of the speckle pattern is related to the changes in the physical properties of the tissue being tested [25]. By recording the temporal speckle pattern, and by using correlation analysis of the video, we can calculate the relative shift between the frames which stands for the temporal oscillation profile. By calculating the Fourier transform of the shifts' vector, the oscillation frequencies of the captured speckle pattern can be computed [26]. The speckles analysis has already been tested successfully for several kinds of measurements such as extraction of multiple speech sources and heartbeats [27], breathing, heart rate, pulse pressure, blood Coagulation, blood oxygenation [28], alcohol concentration [29], detection of pigmented lesions, and human skin hydration [30].

3. Materials and Methods

3.1. The Method of Measurements

The maximal vibration frequency that can be detected by the technique presented above depends on the frame rate of the camera that is used for recording the speckles pattern as a function of time. As we mentioned above, the typical value for Brillouin frequency is about 10 GHz, which is much higher compared to the maximal camera's frame rate. Thus, to detect the backward Brillouin effect by using speckles analysis, we need to find a way to reduce the frequency of the acoustic vibrations. This can be achieved by performing amplitude modulation to the Pump wave. If we modulate the pump with frequency modulation of ω_m we will get two sidebands to the main laser frequency $\omega_{p,0}$ [31]:

$$\omega_{p1} = \omega_{p,0} - \omega_m \tag{3}$$

$$\omega_{p2} = \omega_{p,0} + \omega_m \tag{4}$$

According to Equation (2), for each pump we will get the corresponding acoustic wave, where the frequencies of those waves are given by:

$$\Omega_{B,i} = \frac{2v_a}{c/n}\omega_{p,i} \tag{5}$$

where $i = 0, 1, 2$. For those pump waves we also get the corresponding back-reflected Stokes waves, with frequencies of:

$$\omega_{s,i} = \omega_{p,i} - \Omega_{B,i} \tag{6}$$

B, we also have the cross interaction between each pump wave and the generated Stokes waves of the other pump waves [32]. For example, the cross interaction between pump number 1 with frequency $\omega_{p,1}$ to Stokes number 2 $\omega_{s,2}$ will generate the next acoustic frequency:

$$\Omega_{c,1} = \omega_{p,1} - \omega_{s,2} = \omega_{p,1} - (\omega_{p,2} - \Omega_{B,2}) \tag{7}$$

And by using the Equation (3) we get:

$$\Omega_{c,1} = \Omega_{B,2} - 2 \cdot \omega_m \tag{8}$$

And similarly, it can be shown that the cross interaction between Pump number 2 to Stokes number 1 will generate the next acoustic frequency:

$$\Omega_{c,2} = \Omega_{B,1} + 2 \cdot \omega_m \tag{9}$$

It can be seen from Equation (8) that if we choose the modulation frequency to be very close to the Brillouin frequency $\Omega_{B,2}$ we can get acoustic vibrations with a frequency that may be detected by using our relatively fast (but not 10 GHz fast) camera.

3.2. Experimental Setup

The experimental setup can be seen in Figure 1.

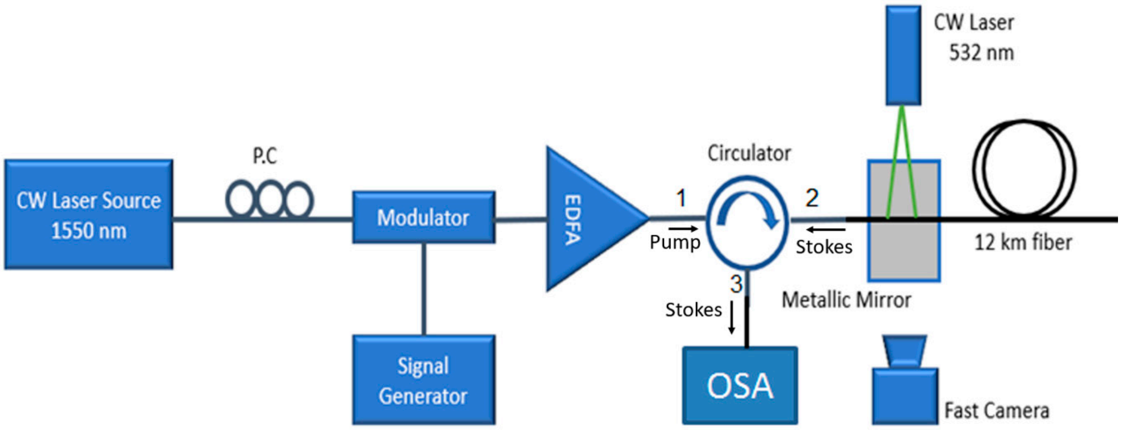

Figure 1. Schematic diagram of the experimental setup. PC: polarization controller; EDFA: Erbium doped fiber amplifier and OSA: optical spectrum analyzer.

A CW-laser with a wavelength of 1550 nm was used as a pump source. To achieve the desired frequency difference, an intensity electro-optic modulator was used, which created two sidebands to the spectrum of the laser source. The modulation frequency was chosen according to the principle that was presented in the previous section according to the camera's frame rate which, in our experiment, was 900 kHz. The Brillouin frequency was approximately found by measuring the frequency shift between the inserted pump wave and the back-reflected Stokes wave. This measurement was performed by using a Fabry Perot scanner with a spectral resolution of about 67 MHz. Since the accepted value was about 10.6 GHz, modulation frequencies around 5.3 GHz were scanned in small steps of 200 khz, to ensure that the generated acoustic frequency will be able to detect by our camera.

The pump waves were amplified by an erbium-doped fiber amplifier (EDFA). The output power of the EDFA was 26 dBm, and it was connected to 12 km single-mode silica fiber via an optical circulator. The core diameter of the fiber was 8 µm and its cladding diameter was 125 µm. The fiber was fixed on a metallic reflector and was illuminated by CW-laser at a wavelength of 532 nm. This illumination passes the fiber cladding and core and due to the reflection at the metallic mirror, a speckle pattern was generated. The illuminated fixed part of the fiber was coiled to many rounds on the reflected surface to increase the interaction between the light and the fiber, and so to enhance the influence of the acoustic vibration on the recorded speckle pattern. The speckle pattern was captured with a high-speed camera (with 128 by 16 pixels) using a 75 mm lens. As we noted above, the camera's frame rate was 900 frames per second.

4. Results

The Pump wave was modulated in amplitude with a frequency of 5.3001 GHz. The spectrum of the input and the back-reflected signals were measured by an optical spectrum analyzer (OSA). Those measurements can be seen in Figure 2.

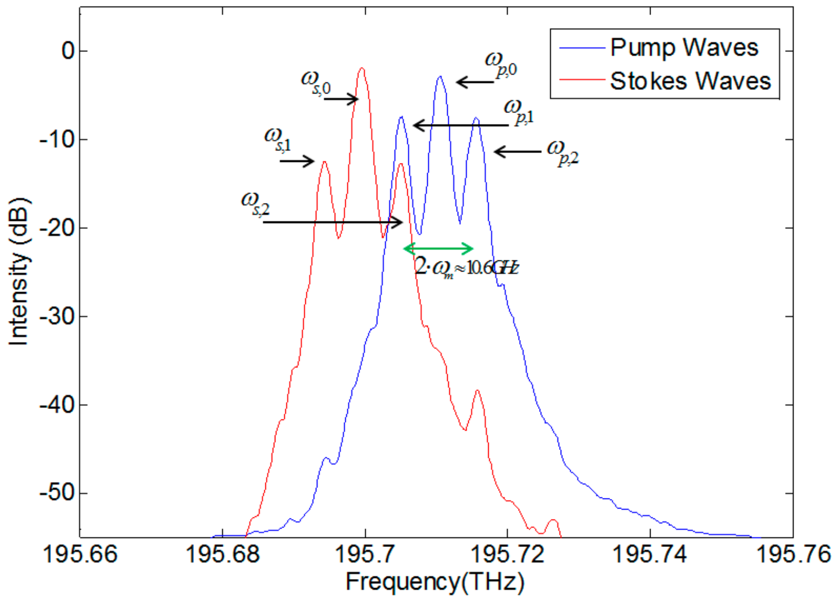

Figure 2. The spectrum of the input (pump waves) and the back-reflected (Stokes waves) signals, measured by optical spectrum analyzer (OSA).

As can be seen in Figure 2, the modulation of the pump created two sidebands to the main wavelength. Accordingly, shifted back-reflected signals were generated for each pump wavelength. Besides the three main peaks of the Stokes signal, some additional peaks at the same positions as those of the pump signal are observed. Those peaks may be caused by leakage of the pump wave via the circulator (from port number 1 to port number 3) or by the Rayleigh scattering of the pump wave. It can also be seen that the accepted shifts in frequencies are about 10.6 GHz, following the typical Brillouin shift value. For each pump wave, the Brillouin frequency shift is slightly different because of the difference in the pump wavelength. Figure 2 illustrates that the frequency of pump number 1 is very close to the frequency of Stoke number 2, which means that their cross interaction yields relatively low acoustic frequency. The main peaks of the pump and the Stokes waves as extracted from Figure 2 can be seen in Table 1.

Table 1. The peak frequencies of the different optical waves in the system.

Wave	Peak (THz)
Pump 0	195.7106
Pump 1	195.7051
Pump 2	195.7156
Stokes 0	195.6995
Stokes 1	195.6944
Stokes 2	195.7051

Then, the speckle pattern was recorded and analyzed for two cases, with and without the above-illustrated pump waves. The accepted results can be seen in Figure 3.

Figure 3 shows the oscillation frequencies of the speckle pattern in the horizontal (X direction) and vertical (Y direction) axes. As can be seen, for the case of the pumped fiber measurement, a peak at frequency 215.2 kHz was obtained. Note that without using pump waves, no frequency peak was accepted, which means the detected peak in the second case was achieved thanks to the acoustic vibrations in the fiber. Then, more modulation frequencies were scanned around the frequency of 5.3 GHz. The results can be seen in Figure 4. Table 2 shows the frequencies of the received peaks that were achieved for each modulation frequency. As can be seen, for each modulation frequency the measured peak was slightly different.

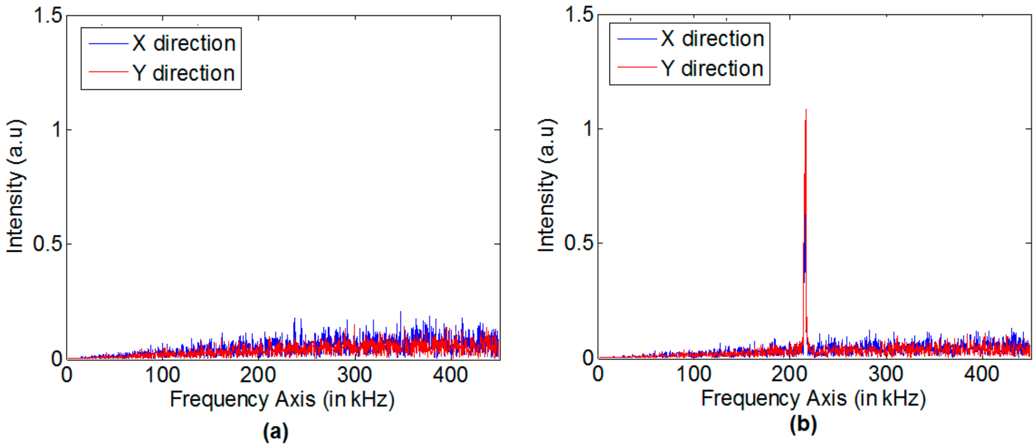

Figure 3. Experimental Results: The oscillation frequencies of the speckle pattern in horizontal (X direction) and vertical (Y direction) axes; (**a**) without pumps and (**b**) with two pump waves.

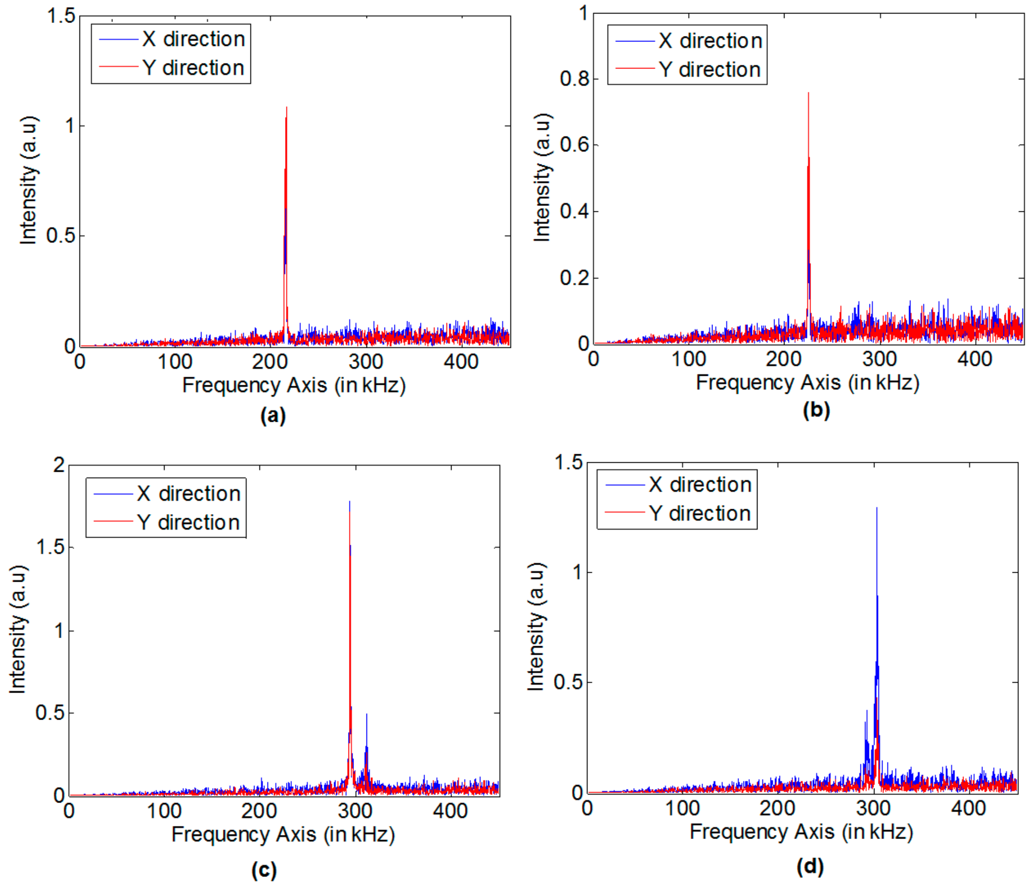

Figure 4. Experimental Results: The oscillation frequencies of the speckle pattern in horizontal (X direction) and vertical (Y direction) axes with pump, with different frequencies of modulation: (**a**) modulation frequency of 5.3001 GHz; (**b**) modulation frequency of 5.3003 GHz; (**c**) Modulation frequency of 5.3005 GHz; and (**d**) modulation frequency of 5.3007 GHz.

Table 2. The peak frequencies received for each modulation frequency.

Modulation Frequency (GHz)	Peak (kHz)
5.3001	215.8
5.3003	225.8
5.3005	294.4
5.3007	303.3

5. Discussion

The results that are presented in Table 2 show that the locations of the measured seem to be not consistent with the changes of the modulation frequencies. According to the relation that is shown in Equation (8), a change of 200 kHz in the modulation frequency should lead to a change of 400 kHz at the measured peak. In our experiment, however, the difference between two consecutive peak values is between 10–68 kHz. However, the accepted results could be well explained by the aliasing phenomena, which cause different signals to become indistinguishable when sampled. Since changes of 400 kHz at the acoustic frequency can take us out of the sampling range (i.e., 450 kHz), the measured frequency Ω_{meas} will be given by the modulo operation in the following way:

$$\Omega_{meas} = \mathrm{mod}(\Omega_{c,1}, 450\mathrm{kHz}) = \mathrm{mod}(\Omega_{B,2} - 2 \times \omega_m, 450\mathrm{kHz}) \tag{10}$$

It can be easily seen that for this relation, a change of 400 kHz in the acoustic frequency $\Omega_{c,1}$ leads to a change of 50 kHz at the measured frequency. This is quite close to the accepted results presented in Table 1 in which the difference between two consecutive peak values is between 10–68 kHz. To clarify this claim, suppose the first frequency peak in the table was sampled without aliasing. According to Equation (8), we can extract the acoustic frequency $\Omega_{B,2}$:

$$\Omega_{B,2} = 2 \times \omega_m + \Omega_{c,1} \tag{11}$$

Which yields:

$$\Omega_{B,2} = 2 \times 5.3001 \times 10^9 + 215.8 \times 10^3 = 10.6004\mathrm{GHz} \tag{12}$$

If we put this value in Equation (10) together with the different modulation frequencies, we could find the theoretical values that should be measured in our experiment. Those values compared to experimental values are presented in Table 3.

Table 3. The measured peak frequencies compare to the theoretical values.

Modulation Frequency (GHz)	Measured Peak (kHz)	Theoretical Value (kHz)
5.3001	215.8	215.8
5.3003	225.8	265.8
5.3005	294.4	315.8
5.3007	303.3	355.8

The small differences between the theoretical values to the experimental results may be explained by small changes in temperature that occurred during the measurement. Equation (10) shows that the measured frequency depends not only on the modulation frequency but also depend on the acoustic frequency $\Omega_{B,2}$. According to Equation (5), this frequency depends on the acoustic velocity, which is a temperature-depended parameter. From both Equation (5) and Equation (10) it is possible to show that a small change of 0.01 m/s in the acoustic velocity leas to change of about 40 kHz in the measured peak, which may explain the small inconsistent of the accepted results.

Note that in our experimental setup there are some additional acoustic frequencies, besides the frequency presented in Equation (7) that may also be detected by our system. Those frequencies include the whole possible combinations of frequencies presented in Equation (5) and the second cross interaction frequency presented in Equation (9), where some of them may be found within the sampling rates or may be detected by the aliasing phenomena. The existence of these additional acoustic frequencies in our system may also be the reason for the secondary peaks accepted in some measurements (see Figure 4c,d). More experimental work is required to find the exact significance of the vibrations which were measured in this setup.

6. Conclusions

In this paper we demonstrated the ability to sense acoustic vibrations in optical fibers resulting from the Brillouin effect by temporal tracking of back-reflected speckle patterns. By using two pump waves in the same fiber, acoustic vibrations that were generated by the cross interaction between the first pump and the Stokes wave of the second pump were apparently detected. In future works, this new detection modality could be used for a realization of improved Brillouin fiber sensors, with high spatial resolution and with shorter measurement time.

Author Contributions: Methodology, S.A. and B.L.; Investigation, B.L.; Supervision, M.S. and Z.Z.; Writing—original draft, S.A.; Writing—review & editing, Z.Z. All authors have read and agreed to the published version of the manuscript.

Funding: This research was funded by the Erlangen Graduate School in Advanced Optical Technologies (SAOT) by the German Research Foundation (DFG) in the framework of the German excellence initiative.

Conflicts of Interest: The authors declare no conflict of interest.

References

1. Chiao, R.Y.; Townes, C.H.; Stoicheff, B.P. Stimulated Brillouin scattering and coherent generation of intense hypersonic waves. *Phys. Rev. Lett.* **1964**, *12*, 592. [CrossRef]
2. Brewer, R.G.; Rieckhoff, K.E. Stimulated Brillouin scattering in liquids. *Phys. Rev. Lett.* **1964**, *13*, 334. [CrossRef]
3. Tang, C.L. Saturation and spectral characteristics of the Stokes emission in the stimulated Brillouin process. *J. Appl. Phys.* **1966**, *37*, 2945–2955. [CrossRef]
4. Ippen, E.P.; Stolen, R.H. Stimulated Brillouin scattering in optical fibers. *Appl. Phys. Lett.* **1972**, *21*, 539–541. [CrossRef]
5. Cotter, D. Stimulated Brillouin scattering in monomode optical fiber. *J. Opt. Commun.* **1983**, *4*, 10–19. [CrossRef]
6. Agrawal, G.P. *Nonlinear Fiber Optics*, 4th ed.; Academic Press: Rochester, NY, USA, 2008; pp. 329–333.
7. Boyd, R.W. *Nonlinear Optics*, 3th ed.; Academic Press: Rochester, NY, USA, 2008; pp. 429–440.
8. Stone, J.; Chraplyvy, A.R. Spontaneous Brillouin noise in long-distance high-bandwidth optical-fibre transmission. *Electron. Lett.* **1983**, *19*, 275–277. [CrossRef]
9. Tkach, R.W.; Chraplyvy, A.R.; Derosier, R.M. Spontaneous Brillouin scattering for single-mode optical-fibre characterisation. *Electron. Lett.* **1986**, *22*, 1011–1013. [CrossRef]
10. Tanemura, T.; Takushima, Y.; Kikuchi, K. Narrowband optical filter, with a variable transmission spectrum, using stimulated Brillouin scattering in optical fiber. *Opt. Lett.* **2002**, *27*, 1552–1554. [CrossRef]
11. Olsson, N.; Van Der Ziel, J. Characteristics of a semiconductor laser pumped Brillouin amplifier with electronically controlled bandwidth. *J. Lightwave Technol.* **1987**, *5*, 147–153. [CrossRef]
12. Thévenaz, L.; Nikles, M.; Fellay, A.; Facchini, M.; Robert, P.A. Applications of distributed Brillouin fiber sensing. In Proceedings of the International Conference on Applied Optical Metrology, Balatonfured, Hungary, 8–11 June 1998; pp. 374–382.
13. Kurashima, T.; Horiguchi, T.; Izumita, H.; Furukawa, S.I.; Koyamada, Y. Brillouin optical-fiber time domain reflectometry. *IEICE Trans. Commun.* **1993**, *76*, 382–390.
14. Kurashima, T.; Horiguchi, T.; Tateda, M. Distributed-temperature sensing using stimulated Brillouin scattering in optical silica fibers. *Opt. Lett.* **1990**, *159*, 1038–1040. [CrossRef] [PubMed]
15. Thévenaz, L. Brillouin distributed time-domain sensing in optical fibers: State of the art and perspectives. *Front. Optoelectron. China* **2010**, *3*, 13–21. [CrossRef]

16. Lecoeuche, V.; Webb, D.J.; Pannell, C.N.; Jackson, D.A. Transient response in high-resolution Brillouin-based distributed sensing using probe pulses shorter than the acoustic relaxation time. *Opt. Lett.* **2000**, *25*, 156–158. [CrossRef] [PubMed]
17. Garus, D.; Krebber, K.; Schliep, F.; Gogolla, T. Distributed sensing technique based on Brillouin optical-fiber frequency-domain analysis. *Opt. Lett.* **1996**, *21*, 1402–1404. [CrossRef]
18. Asraf, S.; Meiri, A.; Lubat, J.; Shemer, A.; Zalevsky, Z. Brillouin optical spatial Fourier domain analyzer. *Opt. Eng.* **2014**, *54*, 011009. [CrossRef]
19. Song, K.Y.; Chin, S.; Primerov, N.; Thévenaz, L. Time-domain distributed fiber sensor with 1 cm spatial resolution based on Brillouin dynamic grating. *J. Lightwave Technol.* **2010**, *28*, 2062–2067. [CrossRef]
20. Hotate, K.; Hasegawa, T. Measurement of Brillouin Gain Spectrum Distribution along an Optical Fiber Using a Correlation-Based Technique—Proposal. *Exp. Simul. IEICE Trans. Electron.* **2002**, *83*, 405–412.
21. Hotate, K.; Tanaka, M. Distributed fiber Brillouin strain sensing with 1-cm spatial resolution by correlation-based continuous-wave technique. *IEEE Photonics Technol. Lett.* **2002**, *14*, 179–181. [CrossRef]
22. Song, K.Y.; He, Z.; Hotate, K. Distributed strain measurement with millimeter-order spatial resolution based on Brillouin optical correlation domain analysis and beat lock-in detection scheme. *Opt. Lett.* **2006**, *31*, 2526–2528. [CrossRef]
23. Lengenfelder, B.; Asraf, S.; Ozana, N.; Späth, M.; Schmidt, M.; Zalevsky, Z. Remote detection of Brillouin radial acoustic modes in an optical fiber using speckle-sensing. In Proceedings of the 26th International Conference on Optical Fiber Sensors, Lausanne, Switzerland, 24–28 September 2018. [CrossRef]
24. Goodman, J.W. Some fundamental properties of speckle. *J. Opt. Soc. Am.* **1976**, *66*, 1145–1150. [CrossRef]
25. Zalevsky, Z.; Garcia, J. Motion Detection System and Method. U.S. Patent 8638991B2, 28 January 2014.
26. Bishitz, Y.; Ozana, N.; Schwarz, A.; Beiderman, Y.; Garcia, J.; Zalevsky, Z. Optical configuration of pigmented lesion detection by frequency analysis of skin speckle patterns. *Biomed. Opt. Express* **2016**, *7*, 1003–1014. [CrossRef]
27. Zalevsky, Z.; Beiderman, Y.; Margalit, I.; Gingold, S.; Teicher, M.; Mico, V.; Garcia, J. Simultaneous remote extraction of multiple speech sources and heart beats from secondary speckles pattern. *Opt. Express* **2009**, *17*, 21566–21580. [CrossRef]
28. Ozana, N.; Margalith, I.; Beiderman, Y.; Kunin, M.; Campino, G.A.; Gerasi, R.; Garcia, J.; Mico, V.; Zalevsky, Z. Demonstration of a Remote Optical Measurement Configuration That Correlates With Breathing, Heart Rate, Pulse Pressure, Blood Coagulation, & Blood Oxygenation. *Proc. IEEE* **2015**, *103*, 248–262.
29. Shenhav, A.; Brodie, Z.; Beiderman, Y.; Garcia, J.; Mico, V.; Zalevsky, Z. Optical sensor for remote estimation of alcohol concentration in blood stream. *Opt. Commun.* **2013**, *289*, 149–157. [CrossRef]
30. Kelman, Y.T.; Asraf, S.; Ozana, N.; Shabairou, N.; Zalevsky, Z. Optical tissue probing: Human skin hydration detection by speckle patterns analysis. *Biomed. Opt. Express* **2019**, *10*, 4874–4883. [CrossRef]
31. Nikles, M.; Thevenaz, L.; Robert, P.A. Brillouin gain spectrum characterization in single-mode optical fibers. *J. Lightwave Technol.* **1997**, *15*, 1842–1851. [CrossRef]
32. Lichtman, E.; Friesem, A.A.; Waarts, R.G.; Yaffe, H.H. Stimulated Brillouin scattering excited by two pump waves in single-mode fibers. *J. Opt. Soc. Am. B* **1987**, *4*, 1397–1403. [CrossRef]